*Landslides and Engineered Slopes. Experience, Theory and Practice – Aversa et al. (Eds)*
*© 2016 Associazione Geotecnica Italiana, Rome, Italy,**ISBN 978-1-138-02988-0*

# Simulated effect of topography and soil properties on hydrologic response and landslide potential under variable rainfall conditions in the Oregon Coast Range, USA

B.B. Mirus, J.B. Smith, J.W. Godt, R.L. Baum & J.A. Coe
*U.S. Geological Survey, Landslide Hazards Program, Golden, Colorado, USA*

ABSTRACT: In the steep, rugged terrain of the Oregon Coast Ranges (USA), heavy precipitation often triggers numerous shallow landslides. While it is well documented that wet antecedent soil-moisture conditions, intense or sustained rainfall, and steep, convergent topography provide the necessary conditions for slope failure, it is difficult to predict exactly when and where landslides will occur. The long-term objective of this study is to improve quantitative characterization of the hydrologic conditions leading to weather-induced landslides in the Oregon Coast Range. The work presented here uses a distributed numerical model of 3D variably saturated subsurface flow, coupled with the infinite-slope stability model to evaluate the effect of topography and soil conditions on landslide potential under variable rainfall conditions. The modeling relies on observations from a well-characterized zero-order basin in the Elliott State Forest for model parameterization and performance evaluation.

## 1 INTRODUCTION

In mountainous terrain, heavy precipitation on already wet hillslopes can result in shallow landslides, which pose a major threat to life and property. Topographic index models can provide broad insights into the spatial distribution of steep, convergent slopes that are most susceptible to such weather-induced landslides (e.g. Dietrich et al. 1995). Additionally, empirical rainfall thresholds gleaned from landslide inventories can be combined with precipitation forecasts to provide some region-specific warning for times of increased landslide potential (Baum & Godt, 2010). However, it remains difficult to simultaneously predict when and where individual weather-induced landslides will occur, due in part to the complexity of subsurface hydrologic-response processes in the heterogeneous near-surface.

It is widely understood that topography, soil thickness and hydraulic properties, rainfall intensity and duration, vegetation characteristics, and antecedent moisture conditions all have a combined influence on near-surface hydrologic response. When infiltration and lateral flow accumulation exceeds drainage, decreased suction stress and/or pore-pressure can subsequently trigger slope failures. These variable influences on hydrologic response and slope stability present a challenge to quantifying the controls on weather-induced landslide initiation at individual locations. It is also difficult to establish a-priori which measurements are most important for developing predictive tools (e.g. landslide warning systems) for a given region. One promising approach to addressing these knowledge gaps is physically based modeling. With this approach, numerical solutions to the physical equations governing subsurface water flow approximate the spatially and temporally variable evolution of pore-pressure responses to rainfall, which in turn can be coupled with a limit equilibrium approach to estimate the factor of safety or likelihood of slope failure for a region of interest (e.g. Baum et al. 2002).

The primary challenge with applying any distributed hydrologic model for slope stability assessments is the difficulty in obtaining adequate data for model parameterization and performance evaluation (Loague et al. 2006). Knowledge of the spatial variations in hydraulic properties in the subsurface is required to parameterize physically based models, and distributed hydrologic response monitoring is also needed to evaluate model performance. Additionally, complete representation of variably saturated subsurface fluid flow in Three Dimensions (3D) is computationally expensive. As a result, many physically based hydrologic models applied to slope stability assessments over broad areas necessarily employ major assumptions to simplify heterogeneity, reduce dimensionality, and/or use approximations of non-linear unsaturated zone flow processes. Despite these challenges, a few previous studies have used comprehensive hydrologic models of fully 3D variably saturated subsurface flow, coupled with a

slope stability model to assess rainfall-induced landslide potential (e.g. Mirus et al. 2007; Simoni et al. 2008; BeVille et al. 2010; Ebel et al. 2010). However, as a result of the aforementioned challenges with data availability and computational burdens, insights from such simulation-based efforts are often limited to the nuances of an individual site and/or only for the short period of time when monitoring data are available.

In this study, we present preliminary results of our research to improve quantitative characterization of the physical controls on shallow landslides in the Pacific Northwest region of the continental USA. The long-term objective of this effort is to use concept-development simulations with a comprehensive physically based hydrologic model (e.g. Loague et al. 2006; Mirus & Loague, 2013) to evaluate the controls on landslide initiation over a range of physically realistic environmental conditions. In this paper, we focus on the initial steps of parameterization and evaluation of a comprehensive physically based model for the Knife Ridge basin in the Elliott State Forest, situated in the Oregon Coast Range, USA. Establishing a realistic model of this well-characterized monitoring site will provide the foundation for subsequent exploration of the combined influence of rainfall, soils, antecedent conditions, and vegetation on slope stability.

## 2 PHYSIOGRAPHIC SETTING

### 2.1 *Oregon Coast Range*

The Oregon Coast Range (OCR) trends north-south along the western part of the state of Oregon, USA (Fig. 1). The climate is strongly influenced by the Pacific Ocean with a rainy season that extends from October to May and a drier season from June through September. In the rugged, forested terrain of the OCR diffusive-type sediment transport processes (i.e. rainsplash, tree throw, and bioturbation) move detached sediment from the largely convex and planar hillslopes into concave hollows (Roering et al. 1999). This diffusive-type transport of sediment results in a spatially variable distribution of colluvium (or soil mantle) that is thinnest along ridge lines and becomes progressively thicker downslope. Since rainfall readily infiltrates into these highly permeable hillslopes, the erosion and transport of sediment by overland flow on hillslopes is not common in the OCR. Instead, subsurface stormflow moves laterally, converging in unchanneled hollows, where the locally accumulated sediment is periodically evacuated by discrete slope failures (i.e. landslides).

The steep hillslopes and heavy wet-season precipitation in the OCR make it highly prone to the hydrologic conditions that trigger such shallow slope failures and thus the OCR provides an ideal natural setting to study weather-induced landslides. Additionally, slope instability is further promoted by human activities such as timber harvesting (Swanson & Dyrness, 1975; Schmidt et al. 2001; Roering et al. 2003) and road construction (Swanson & Dyrness, 1975; Mirus et al. 2007). Thus, it is also important to understand the potential differences in landslide triggering between natural and disturbed basins.

Although topography, geology, soil properties, and anthropogenic disturbances predispose certain locations to landslides, it is the periods of high-intensity and/or long-duration rainfall that exert the dominant control on the timing of landslide initiation in the OCR. For example, major storms in February and November of 1996 with mean rainfall intensities of 4.9 mm/hr (71 hr duration) and 3.4 mm/hr (39 hr duration), respectively, initiated numerous landslides across the region (Robison et al. 1999; Montgomery et al. 2009; Coe et al. 2011). Thus, characterizing hydrologic-response dynamics under such extreme rainfall conditions is a research priority.

### 2.2 *Elliott State Forest*

The Elliott State Forest covers 376 km$^2$ in the OCR (Fig. 1). The annual precipitation ranges from 1,500 mm at lower elevations up to 3,000 mm at higher elevations (Andrus et al. 2003). In 2009, the U.S. Geological Survey (USGS) began installation of systems to monitor precipitation and shallow hillslope hydrologic conditions in several landslide-prone basins within the Elliott State Forest. The primary objective of this monitoring was to

Figure 1. Regional map of study area in the Elliott State Forest, Oregon Coast Range, Oregon, USA.

improve empirical understanding of how antecedent soil-moisture conditions and rainfall intensity and duration relate to landslide initiation. A secondary objective was to provide continuous observations to test regional and site-specific hydrologic and slope-stability models.

### 2.2.1 *Knife ridge monitoring site*

One of the USGS monitoring sites is located below Knife Ridge in a southwest-facing zero-order basin (see Smith et al. 2014). The drainage area of the basin is about 18,000 m$^2$, but only the potential landslide source area in the upper 4,350 m$^2$ is instrumented with monitoring equipment (Fig. 2). This unchanneled basin was selected because it had been recently logged, the hillslopes are quite steep (greater than 30°), and the site is also accessible by a forest road at the upper drainage divide. The basin and surrounding area was clear-cut logged in 2005 and then replanted with Douglas fir (*Pseudotsuga menzeisii*) shortly thereafter. Although Knife Ridge was believed to be highly prone to failure, the site has not yet been subject to any landslides since logging took place.

The site characterization and monitoring data are well suited to the parameterization and evaluation of a comprehensive physically based hydrologic model. The basin was surveyed with a total station in April 2009. The surveyed point density was sufficient to produce a topographic map with a 1-m contour interval. Eight soil pits were excavated to assess the stratigraphy within the colluvium and to collect samples for grain-size and laboratory analyses of hydraulic and geotechnical properties. The instrumentation includes three inclinometers, two tipping-bucket rain gages, four shallow piezometers, and eight sets of nested volumetric water content and pore-pressure sensors (Fig. 2). The nested water-content and pressure sensors were installed at three different depths within each of the eight soil pits to constrain vertical fluxes. For the simulations presented here, we use the precipitation and hydrologic-response data from October 2009 to October 2012.

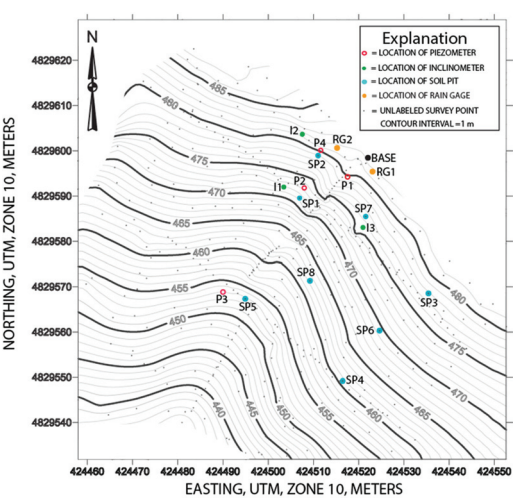


Figure 2. Topography and instrument locations at the Knife Ridge Monitoring Site (from Smith et al. 2014).

## 3 METHODOLOGY

### 3.1 *Integrated hydrology model*

The physically based Integrated Hydrology Model (InHM) was designed to simulate 3D variably saturated flow and solute transport in porous media and macropores, fully coupled with 2D flow and transport over the land surface (VanderKwaak, 1999). InHM has been successfully employed for catchment scale, event-based rainfall-runoff simulation (VanderKwaak & Loague, 2001; Ebel et al. 2007; Mirus and Loague, 2013), long-term, continuous hydrologic-response simulations (Heppner et al. 2007; Ebel et al. 2008; Mirus et al. 2011a; Mirus 2015), and slope stability assessments (Mirus et al. 2007; BeVille et al. 2010; Ebel et al. 2010). The depth-integrated shallow water equations, advection-dispersion equation, and the surface/subsurface coupling scheme in InHM were not applied in this study and thus are described elsewhere (VanderKwaak and Loague, 2001). InHM estimates $\vec{q}$ = subsurface flow [m s$^{-1}$] as:

$$\vec{q} = -k_{rw} \frac{\rho_w g}{\mu_w} \vec{k} \Delta(\psi + z) \tag{1}$$

where $k_{rw}$ = relative permeability [–]; $\rho_w$ = density of water [kg m$^{-3}$]; $g$ = gravitational acceleration [m s$^{-2}$]; $\mu_w$ = dynamic viscosity of water [kg m$^{-1}$ s$^{-1}$]; $\vec{k}$ = intrinsic permeability vector [m$^2$]; $\psi$ is the pressure head [m]; and $z$ is the elevation [m]. The relationship between intrinsic permeability and $K_s$ = saturated hydraulic conductivity [m s$^{-1}$] is:

$$K_s = k \frac{\rho_w g}{\mu_w} \tag{2}$$

The relationship between pressure head and $p$ = pore-water pressure [kg m$^{-1}$ s$^{-2}$] is:

$$p = \rho_w g \psi \tag{3}$$

InHM solves the physical equations for fluid flow (e.g. Equ. 1) using the finite element method with adaptive time steps. The finite element mesh we devel-

oped for Knife Ridge consists of 2,051 surface and 135,366 subsurface nodes (Fig. 3). Horizontal nodal spacing ranges from 1 m in the hollow to 2 m along the drainage divides; vertical spacing ranges from 0.02 m in the near surface to 2 m at depth (Fig. 3).

### 3.2 *Soil hydraulic properties*

Based on the detailed site characterization of the colluvium (Smith et al. 2014) we parameterized three hydrostratigraphic units (Fig. 4). From the land surface down, these uniform, homogeneous, isotropic units include: (1) organic-rich layer of sandy litter and duff, (2) cobble-rich sandy colluvium, and (3) weathered sandstone. For each of these three hydrostratigraphic units, InHM requires the user to define $b$ = thickness [m], as well as parameter values for $K_s$, $\theta_s$ = porosity [$m^3$ $m^{-3}$], $\theta_r$ = residual water content [$m^3$ $m^{-3}$], and van Genuchten (1980) parameters $\alpha$ [$m^{-1}$] and $n$ [-] to defining soil-water retention and unsaturated hydraulic conductivity relations.

The hydraulic parameter values are physically constrained by the results from previous laboratory analyses of core samples using the TRIM method (Wayllace & Lu, 2012) and inverse modeling of the 2009–2012 in-situ monitoring data. However, a detailed comparison of these two-parameter estimation methods at Knife Ridge has revealed notable differences, as well as considerable spatial variability and hysteretic wetting and drying properties (Brian Ebel, written communication). Similarly, results from ponded infiltration experiments and mini-disk infiltrometer tests, which we conducted at Knife Ridge in July 2015, suggest that estimates of $K_s$ at the soil surface can vary over an order of magnitude depending on the measurement technique. We attribute these variations to the influence of near-surface macropores and heterogeneous soil structures we observed there, which should be taken into account when parameterizing the soil hydraulic properties (Mirus, 2015). Regardless, we used these laboratory and in-situ analyses (Brian Ebel, written communication) combined with our recent field measurements to constrain effective hydraulic properties for the hydrostratigraphic units (Table 1). Additionally, although InHM was modified to consider the impact of hysteresis (Ebel et al. 2010), at this stage in the model parameterization and validation, we use non-hysteretic water retention curves and follow the recommendation of Ebel et al. (2010) by using in-situ wetting measurements for constraining $\alpha$ and $n$.

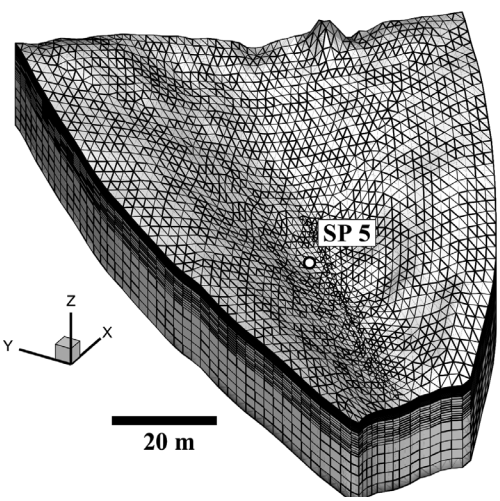


Figure 3. Finite element mesh and the location of nested simulated observation nodes at Soil Pit #5 (SP5). Note: the X-direction is Northing and the Y-direction is Easting (see Fig. 2).

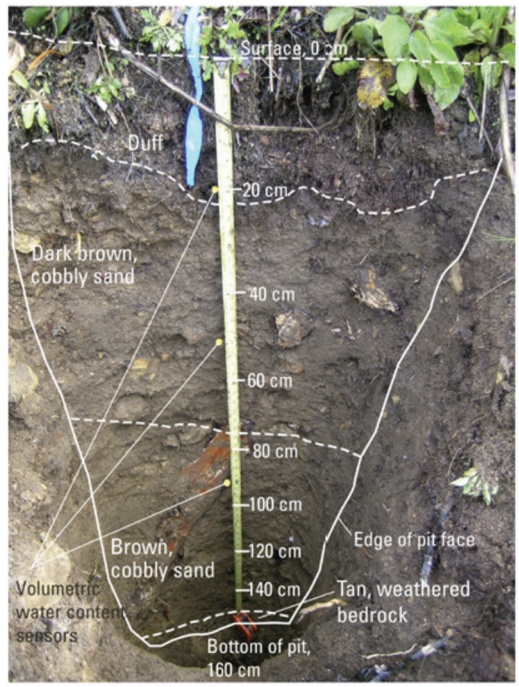


Figure 4. Example soil pit used to define the hydrostratigraphic units applied in the InHM simulations and location of water-content sensors used to evaluate model performance (SP2 from Smith et al. 2014).

### 3.3 *Boundary conditions*

The lateral and upper drainage divides (Fig. 3) are no flow boundaries. The basal boundary condition

Table 1. Parameterization of the hydrostratigraphic model units for Knife Ridge.

| Unit | b (m) | $K_s$ (m s$^{-1}$) | $\theta_s$ (m$^3$ m$^{-3}$) | $\theta_r$ (m$^3$ m$^{-3}$) | $\alpha$ (m$^{-1}$) | n (–) |
|---|---|---|---|---|---|---|
| Sandy duff | 0.2 | $3.0 \times 10^{-4}$ | 0.38 | 0.14 | 7.6 | 1.3 |
| Cobbly Sand | 1.8 | $1.0 \times 10^{-6}$ | 0.32 | 0.15 | 9.6 | 1.7 |
| Sandstone | 18.0 | $1.2 \times 10^{-8}$ | 0.25 | 0.01 | 4.3 | 1.2 |

allows free drainage at a unity vertical hydraulic gradient. The downgradient boundary condition allows lateral drainage at rates proportional to the local hydraulic gradient, which is calculated across this subsurface boundary based on a user-defined hydraulic head at a point outside the model domain (see Heppner et al. 2007). We defined this local head using a constant pressure head value of 1.0 at the point where a perennial channel emerges at the basin outlet. For the time-variable applied flux boundary conditions across the land surface, we employed local and site-specific climatic forcing data, as described below.

### 3.4 *Climatic forcing data*

The precipitation forcing data consist of hourly rainfall intensities aggregated from tipping-bucket rain gages. However, no site-specific data were collected at Knife Ridge to constrain the temporal variability in evapotranspiration (ET). Instead, we used monthly averages from evaporation pan data at the nearby Fern Ridge Dam (Western Regional Climate Center, http://www.wrcc.dri.edu), which we take as representative of the monthly potential ET. We disaggregated those monthly totals into hourly rates during daylight hours, which InHM takes as a potential sink term across the land surface. Field observations from soil pit excavations at Knife Ridge (Smith et al. 2014) suggest that roots are most common in the upper portions of the sandy colluvium profile, so we assume an effective rooting depth of 1.2 m. InHM uses the potential ET time-series and available soil moisture within this specified rooting-depth to calculate actual ET fluxes in the simulations.

### 3.5 *Initial conditions*

We followed the warm-up simulation protocol used in previous applications of InHM (e.g. Mirus et al. 2011b) to establish internally valid initial conditions. Our warm-up protocol for Knife Ridge consisted of a 600-day simulation in which the basin was drained from near-saturation (i.e. initial total head values set equal to 99% of the elevation head throughout the domain). During the 600 days of drainage a continuous low-intensity rainfall ($1.0 \times 10^{-9}$ m s$^{-1}$) was applied from days 1 through 120, whereas no rainfall or ET was applied from days 121 through 600. At the conclusion of this warm-up simulation, the steady-state water-table elevation and simulated soil water contents were in close agreement with the observations at the end of the dry season in both the piezometers (i.e. greater than 3.0 m below the land surface) and volumetric water content sensors (i.e. approximately 0.20, which is very close to the colluvium $\theta_r$ values).

### 3.6 *Infinite slope model*

Although it has been demonstrated that landslides can occur under unsaturated conditions (Godt et al. 2009) due to a reduction in suction stress (e.g. Lu et al. 2010), our initial efforts here use the infinite slope model assuming that saturated conditions are necessary to elevate pore pressures and initiate failure. Assuming a continuous phase of pore-air pressure, equal to atmospheric pressure, the infinite slope model, as employed here, estimates the Factor of Safety (*FS*) as:

$$FS = \frac{(C' + \Delta C) + \left(\gamma_t z_{uz} cos^2\beta - pS\right) tan\varphi'}{\gamma_t z_{uz} \beta sin\beta} \tag{4}$$

where $C'$ = effective soil cohesion [kg m$^{-1}$ s$^{-2}$]; $\Delta C$ = root cohesion [kg m$^{-1}$ s$^{-2}$]; $\gamma_t$ = total unit weight of the soil [kg m$^{-w}$ s$^{-2}$]; $z_{uz}$ = unsaturated soil thickness [m]; $\beta$ = slope angle [º]; $\varphi$ = angle of internal friction [º]; $S$ = saturation [m$^3$ m$^{-3}$], and $S$ is the $\theta$ = soil water content divided by porosity, $\theta_s$. The value of $\beta$ is taken as the local slope at the point of interest and temporally variable values of $\theta$ are simulated by InHM. The parameter values we used for the remaining geotechnical properties are summarized in Table 2. For the analysis presented here, we assume the potential failure plane for shallow landslides at Knife Ridge would occur at the interface between the colluvium and the underlying weathered sandstone bedrock, and focus on calculating the time-series of *FS* at the location of SP5 in the basin axis (Fig. 2).

Table 2. Soil geotechnical properties used in the infinite slope model (from Ebel et al. 2010).

| Parameter | $C'$ (kPa) | $\Delta C$ (kPa) | $\gamma_t$ (kN m$^{-3}$) | $\varphi'$ (º) |
|---|---|---|---|---|
| | 0.9 | 0.1 | 15.7 | 40 |

## 4 RESULTS AND DISCUSSION

InHM-simulated output includes distributed pressure heads and volumetric water contents at all 135,366 nodes in the finite element mesh (Fig. 3) for every time step during the 3-year simulation period. It is impractical to show a comprehensive summary of all this model output here, so we focus on a selection of the output in two formats: (1) comparison of continuous time-series of observed and simulated hydrologic response at discrete locations, and (2) snapshots of distributed state variables throughout the model domain at discrete times. The time-series include soil water content (Fig. 5) and pore pressures (Fig. 6) at multiple depths within SP5, which is located in the convergent hollow, where landslide initiation would be most likely. The snapshots include the distribution of pore-pressures across the base of the colluvium above the weathered sandstone bedrock (Fig. 7) and a cross-section through the hollow axis showing saturation in the subsurface (Fig. 8), on March 2, 2010, which corresponds to the time when peak pore pressure was recorded in the deepest tensiometer in the basin, when landslide initiation would be most likely.

### 4.1 *Observed vs. simulated hydrologic response*

Comparison of the observed and InHM-simulated time-series of volumetric water contents (Fig. 5) and pore pressures (Fig. 6) reveals that the model captures the dynamics in the near-surface (20, 50, 59, and 129 cm), but tends to over-predict the response at greater depths (160 and 271 cm). This may be due largely to inadequate representation of the geometry of the interface between the colluvium and underlying weathered bedrock. Small bedrock depressions can control thresholds for lateral subsurface stormflow (e.g. Tromp-van Meerveld & McDonnell, 2006), which can contribute to pore-pressure response. However, since the hydrostratigraphic units in in our current InHM simulations for Knife Ridge are uniform, the bedrock topography is defined by the surface topography. This uniform thickness of the colluvium (i.e. sandy duff and cobbly sand units in Table 1) is based on the limited depth measurements reported by Smith et al. (2014), whereas geophysical surveys at Knife Ridge suggest that there may be some sig-

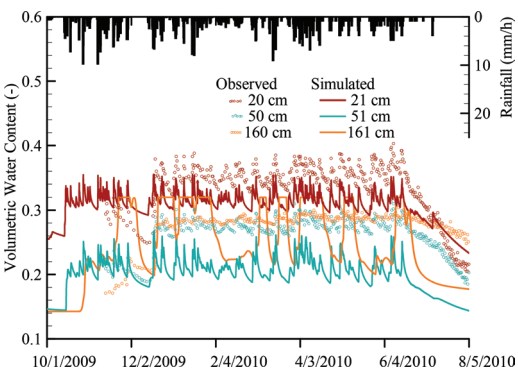


Figure 5. Rainfall hyetograph and observed and InHM-simulated time-series of volumetric water contents at SP5 during October 1, 2009 through August 5, 2010.

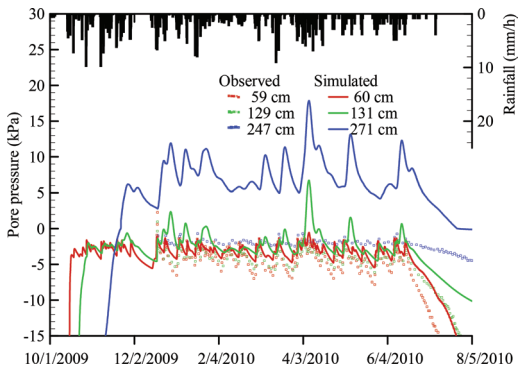


Figure 6. Rainfall hyetograph and observed and InHM-simulated time-series of pore pressures at SP5 during October 1, 2009 through August 5, 2010.

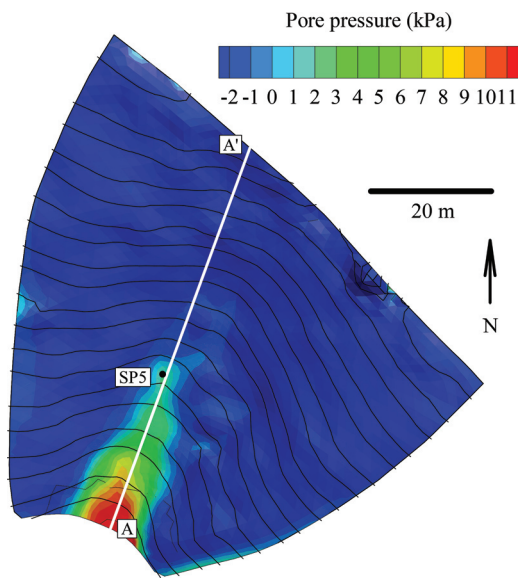


Figure 7. Snapshot of InHM simulated pore-pressure distributions on March 2, 2010 at 9:00 am, at the interface between the colluvium and the weathered bedrock, 2.0 m, below land surface. Contour lines show surface (and bedrock) topography with 2.0 m intervals. The white line (A-A') shows the position of the cross-section (Fig. 8).

nificant bedrock depressions (Morse et al. 2012). We plan to refine the InHM simulations to account for this more complex bedrock topography and the variations in colluvium thickness, from thinnest along ridgelines to thickest in the hollow axis. We anticipate that these changes will improve model performance at depth.

The depth-dependent model performance issues may also be indicative of the contrast between the detailed characterization of the colluvium with analysis of laboratory and in-situ data (Brian Ebel, written communication), and the relative lack of site-specific data to characterize the weathered bedrock. However, since it was not feasible to install any of the instruments into the weathered bedrock itself, it may be challenging to improve parameterization and evaluate model performance at depths below the base of the colluvium.

Given our simplified representation of the stratigraphy, the lack of data on the sandstone bedrock at Knife Ridge, and our crude approximation of the potential ET, the minor problems with model performance are not surprising. Previously, performance evaluations of InHM have emphasized quantitative comparisons between simulated and observed surface discharge hydrographs at catchment outlets (Heppner et al. 2007; Mirus et al. 2007). However, as noted by Loague et al. (2006), evaluating this form of integrated catchment response does not guarantee that the model is performing well for the right reasons or capturing the distributed response accurately. Since the monitoring at Knife Ridge includes only subsurface hydrologic response data it is possible to evaluate the distributed response, but not the integrated response and overall mass balance. As such, it is not possible to compare how well InHM performs at Knife Ridge relative to previous applications. One similar location where InHM simulations were rigorously evaluated with both surface and subsurface data was for the nearby CB1 catchment (Ebel et al. 2007, 2008), also located in the OCR. The monitoring efforts at CB1 focused on three artificial sprinkling experiments, but the continuous hydrologic monitoring records included numerous gaps in the data. Whereas the CB1 catchment experienced a catastrophic landslide during the winter of 1996, leading to the termination of monitoring efforts (Montgomery et al. 2009), the continuous and ongoing monitoring efforts at Knife Ridge provide a unique opportunity to further improve and evaluate model performance and test hypotheses related to the controls on shallow landslides.

### 4.2 *Distributed response and slope stability*

Despite some problems with model performance, it is instructive to examine how InHM can provide insights into the potential factors leading to weather-induced landslide initiation. The snapshot of the spatial distribution of simulated pore-pressures at the base of the colluvium during the peak observed response (Fig. 7) illustrates the build-up of excess pore pressures along the axis of the concave hollow (Fig. 8) in response to the lateral subsurface flow convergence from the surrounding planar and convex hillslopes. Similarly, the snapshot of the cross section along the catchment axis showing subsurface saturation illustrates how downslope flow accumulation above the bedrock can explain potential drainage area thresholds for landslide initiation.

Figure 9 shows a time series of the *FS* (Equ. 4) calculated with the InHM simulated output from the node located 2.0 m below the land surface at

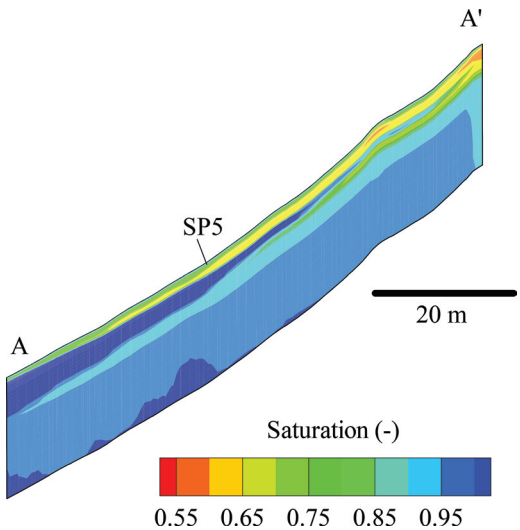


Figure 8. Snapshot of InHM simulated subsurface saturation on March 2, 2010 at 9:00 am, for a 2D cross section along the hollow axis (see Fig. 7).

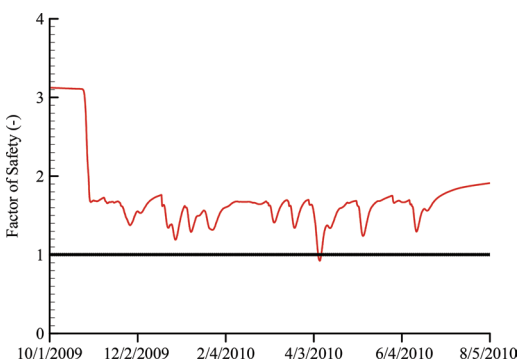


Figure 9. Simulated Factor of Safety (*FS*) at the base of the colluvium in SP5 (Figs. 7 and 8).

SP5 (Figs. 7 and 8). While the basin did not fail during the simulation period and the *FS* estimates suggest the slope is largely stable throughout the wet season, the

*FS* values dip below unity for a brief period in April 2010. This may be a result of over-predictions of pore pressures at depth simulated by the model for the reasons discussed previously. The overestimates of the failure potential could also be due to imprecise estimates of the geotechnical parameters (Table 2), which were based on measurements from a similar site in the OCR (Ebel et al. 2010). Completing laboratory analyses of the samples we collected at Knife Ridge to obtain site specific parameters could improve the accuracy of the slope stability estimates.

## 5 CONCLUSIONS

In this paper we examine the utility of InHM, a physically based model, for addressing knowledge gaps related to the hydrologic controls on weather-induced landslides. We present preliminary steps towards using InHM to examine the influence of soil hydraulic properties, topographic convergence, and dynamic climatic forcing on hydrologic response and slope stability. We successfully apply InHM for the steep, unchannelled Knife Ridge basin in the Oregon Coast Range, USA, where the USGS has conducted long-term monitoring efforts and collected sufficient data to parameterize and evaluate the model. We demonstrate that the InHM simulation results for Knife Ridge compare reasonably well to volumetric water content and pore-pressure time-series within the near surface, which were measured continuously between 2009 and 2012 at multiple depths throughout the basin. We also identify several areas where model performance could be improved. For example, more realistic representation of the bedrock topography and geometry of hydrostratigraphic units should lead to better model performance at greater depths within the colluvium. Having established that InHM is capable of approximating the hydrologic response to rainfall at Knife Ridge, we also demonstrate its utility for developing distributed and continuous assessments of slope stability.

Previous applications of InHM included concept-development simulations to quantify thresholds for runoff-generation and sediment transport over a broad range of environmental and climatic conditions (Mirus & Loague 2013). The parameterization of the current simulations for Knife Ridge (Tables 1 and 2) provide a useful starting point for generating similar concept-development simulations with InHM focused on identifying more general relations between soil-hydraulic properties and rainfall thresholds for landslide initiation.

## REFERENCES


Andrus, C., Bahus, K., Craig, K., Runyon, J., Schwindt, R. & Souder, J. 2003. Elliott State Forest watershed analysis: Oregon Department of Forestry, 288 p.

Baum, R.L. & Godt, J.W. 2010. Early warning of rainfall-induced shallow landslides and debris flows in the USA. *Landslides*, 7 (3): 259–272.

Baum, R.L., Savage W.Z. & Godt, J.W. 2002. TRIGRS—A Fortran program for transient rainfall infiltration and grid-based regional slope-stability analysis. *U.S. Geological Survey Open-File Report* 424, 38.

BeVille, S.H., Mirus, B.B., Ebel, B.A. Mader, G.G. & Loague, K. 2010. Using simulated hydrologic response to revisit the 1973 Lerida Court landslide. *Environmental Earth Sciences*, DOI:10.1007/s12665-010-0448-z.

Coe, J.A., Michael, J.A., & Burgos, M.M. 2011. Map of debris flows caused by rainfall during 1996 in parts of the Reedsport and Deer Head Point quadrangles, Douglas County, Southern Coast Range, Oregon: *U.S. Geological Survey Open-File Report,* 2011–1150, 9 p., 1 map sheet, at *http://pubs.usgs.gov/of/2011/1150/*.

Dietrich W.E., Reiss R., Hsu M.L., & Montgomery D.R. 1995. A process-based model for colluvial soil depth and shallow landsliding using digital elevation data. *Hydrological Processes,* 9: 383–400.

Ebel B.A., Loague K., Montgomery D.R., Dietrich W.E. 2008. Physics based continuous simulation of long-term near-surface hydrologic response for the Coos Bay experimental catchment. *Water Resources Research,* 44:W07417. doi:101029/2007 WR006442.

Ebel B.A., Loague K., VanderKwaak J.E., Dietrich W.E., Montgomery D.R., Torres R., & Anderson S.P. 2007. Near-surface hydrologic response for a steep, unchanneled catchment near Coos Bay, Oregon: 2 physics-based simulations. *American Journal of Science,* 307:709–748. doi:102475/04200703.

Ebel, B.A., Loague, K. & Borja, R.I. 2010. The impacts of hysteresis on variable saturated hydrologic response and slope failure. *Environmental Earth Sciences,* 61: 1215–1225, doi:10.1007/s12665-009-0445-2.

Godt, J.W., Baum, R.L. & Lu, N. 2009, Landsliding in partially saturated materials, *Geophysical Research Lett*ers, 36, L02403, doi:10.1029/2008GL035996.

Heppner, C.S., Loague, K., and VanderKwaak, J.E., 2007, Long-term InHM simulations of hydrologic response and sediment transport for the R-5 catchment: *Earth Surface Processes and Landforms*, doi:10.1002/esp.1474.

Loague K., Heppner C.S., Mirus B.B., Ebel B.A., Ran Q., Carr A.E., BeVille S.H., & VanderKwaak J.E. 2006. Physics-based hydrologic-response simulation: Foundation for hydroecology and hydrogeomorphology. *Hydrological Processes* 20: 1231–1237.

Lu, N., Godt, J.W., & Wu, D.T. 2010. A closed-form equation for effective stress in unsaturated soil, *Water Resour. Res.*, 46, W05515, doi:10.1029/2009 WR008646.

Mirus B.B., Ebel, B.A, Loague, K., & Wemple, B.C. 2007. Simulated effect of a forest road on near-surface

hydrologic response: Redux. *Earth Surface Processes and Landforms* 32: 126–142.

Mirus, B.B, Loague, K., Cristea, N., Burges, S., & Kampf, S. 2011a. A synthetic hydrologic-response dataset. *Hydrological Processes*, DOI:10.1002/hyp.8185.

Mirus, B.B. & Loague, K. 2013. How runoff begins (and ends): Characterizing hydrologic response at the catchment scale. *Water Resources Research,* DOI/10.1002/wrcr.20218.

Mirus, B.B. 2015. Evaluating the importance of characterizing soil structure and horizons in parameterizing a hydrologic process model. *Hydrological Processes,* DOI: 10.1002/hyp.10592.

Mirus, B.B., Ebel, B.A., Heppner, C.S., & Loague, K. 2011b. Assessing the detail needed to capture rainfall-runoff dynamics with physics-based hydrologic-response simulation. *Water Resources Research,* DOI.1029/2010 WR009906.

Montgomery, D.R., Schmidt, K.M., Dietrich, W.E. & McKean, J. 2009. Instrumental record of debris flow initiation during natural rainfall—Implications for modeling slope stability. *Journal of Geophysical Research*, v114, F01031, 16 p.

Morse, M.S., Lu, N., Godt, J.W., Revil, A. & Coe. J.A. 2012. Comparison of soil thickness in a zero-order basin in the Oregon Coast Range using a soil probe and electrical resistivity tomography, *Journal of Geotechnical and Geoenvironmental Engineering*, 138:1470–1482.

Roering, J.J., Kirchner, J.W., & Dietrich, W.E. 1999. Evidence for nonlinear, diffusive sediment transport on hillslopes and implications for landscape morphology, *Water Resources Research*, v. 35, no. 3, p. 853–870.

Roering, J.J., Schmidt, K.M., Stock, J.D., Dietrich, W.E. & Montgomery, D.R. 2003. Shallow landsliding, root reinforcement, and the spatial distribution of trees in the Oregon Coast Range, *Canadian Geotechnical Journal*, v. 40, p. 237–253.

Schmidt, K.M., Roering, J.J., Stock, J.D., Dietrich, W.E., Montgomery, D.R. & Schaub, T. 2001. The variability of root cohesion as an influence on shallow landslide susceptibility in the Oregon Coast Range. *Canadian Geotechnical Journal*, v. 38, p. 995–1024.

Simoni S., Zanotti F., Bertoldi G., & Rigon R. 2008. Modelling the probability of occurrence of shallow landslides and channelized debris flows using GEOtop-FS. *Hydrological Process* 22:532–545.

Smith, J.B., Godt, J.W., Baum, R.L., Coe, J.A., Burns, W.J., Morse, M.M., Sener-Kaya, B., Kaya, M. 2014. Hydrologic monitoring of a landslide-prone hillslope in the Elliott State Forest, Southern Coast Range, Oregon, 2009–2012. *U.S. Geological Survey Open-File Report,* 2013–1283, 66 p.

Swanson F.J & Dyrness C.T. 1975. Impact of clear-cutting and road construction on soil erosion by landslides in the western Cascade Range, Oregon. *Geology* 3: 393–396.

Tromp-van Meerveld, H.J. & McDonnell, J.J. 2006. Threshold relations in subsurface stormflow: 2. The fill and spill hypothesis, *Water Resources Research*, 42, W02411, doi:10.1029/2004 WR003800.

VanderKwaak J.E. & Loague K. 2001. Hydrologic-response simulations for the R-5 catchment with a comprehensive physics-based model. *Water Resources Research* 37: 999–1013.

VanderKwaak J.E. 1999. Numerical simulation of flow and chemical transport in integrated surface-subsurface hydrologic systems. PhD dissertation. University of Waterloo, Waterloo, Ontario, Canada.

Wayllace, A. & Lu, N. 2012. A transient water release and imbibitions method for rapidly measuring wetting and drying soil water retention and hydraulic conductivity functions, *J. ASTM Geotech Test.,* 35, 1–15.

Western Regional Climate Center. Desert Research Institute: http://www.wrcc.dri.edu/htmlfiles/westevap.final.html, last accessed: October 9, 2015.

van Genuchten, MTh. 1980. A closed-form equation for predicting the hydraulic conductivity of unsaturated soils. *Soil Science Society America Journal,* 44: 892–898.